

A Triazole-Containing Metal–Organic Framework as a Highly Effective and Substrate Size-Dependent Catalyst for CO₂ Conversion

Pei-Zhou Li,^{†,||,§} Xiao-Jun Wang,^{†,||,§} Jia Liu,^{‡,||,§} Jie Sheng Lim,[†] Ruqiang Zou,^{*,‡,||} and Yanli Zhao^{*,†,||,#}

[†]Division of Chemistry and Biological Chemistry, School of Physical and Mathematical Sciences, Nanyang Technological University, 21 Nanyang Link, Singapore 637371

[‡]Beijing Key Laboratory for Theory and Technology of Advanced Battery Materials, Department of Materials Science and Engineering, College of Engineering, Peking University, Beijing 100871, China

^{||}Singapore Peking University Research Centre for a Sustainable Low-Carbon Future, 1 Create Way, Singapore 138602

[#]School of Materials Science and Engineering, Nanyang Technological University, 50 Nanyang Avenue, 639798, Singapore

S Supporting Information

ABSTRACT: A highly porous metal–organic framework (MOF) incorporating both exposed metal sites and nitrogen-rich triazole groups was successfully constructed via solvothermal assembly of a clicked octacarboxylate ligand and Cu(II) ions, which presents a high affinity toward CO₂ molecules clearly verified by gas adsorption and Raman spectral detection. The constructed MOF featuring CO₂-adsorbing property and exposed Lewis-acid metal sites could serve as an excellent catalyst for CO₂-based chemical fixation. Catalytic activity of the MOF was confirmed by remarkably high efficiency on CO₂ cycloaddition with small epoxides. When extending the substrates to larger ones, its activity showed a sharp decrease. These observations reveal that MOF-catalyzed CO₂ cycloaddition of small substrates was carried out within the framework, while large ones cannot easily enter into the porous framework for catalytic reactions. Thus, the synthesized MOF exhibits high catalytic selectivity to different substrates on account of the confinement of the pore diameter. The high efficiency and size-dependent selectivity toward small epoxides on catalytic CO₂ cycloaddition make this MOF a promising heterogeneous catalyst for carbon fixation.

Carbon dioxide (CO₂) as the primary anthropogenic gas has been cited as the leading culprit in inducing average temperature increase of the global surface as well as subsequent climate changes.¹ The CO₂ emitted from the power plants actually can be taken as an abundant carbon source. Besides the physical adsorption and permanent underground deposition of CO₂, an alternative and more attractive strategy for addressing anthropogenic CO₂ emission issues should be catalytically chemical conversion of CO₂ into value-added chemicals and materials, so that the emitted CO₂ can be reused in the carbon recycling on the earth.^{2,3} This approach not only reduces the anthropogenic greenhouse gas emission but also generates valuable chemical commodity to decrease our dependence on petrochemicals. Therefore, it should be a reliable way toward a sustainable low-carbon future. Taking account of the issues of the product purifications and catalyst recycling in homogeneous

catalytic processes, some heterogeneous catalysts have been developed for the CO₂ chemical conversion.³

Owing to high porosity, adjustable compositions, and decorative pore surface, metal–organic frameworks (MOFs) have emerged as highly promising materials for wide applications, including the adsorption and separation of small molecules such as H₂,⁴ CH₄, and other hydrocarbons^{5,6} as well as CO₂.¹ Recently, MOFs have also been demonstrated as efficient catalysts in heterogeneous catalytic reactions.⁷ Although some MOFs have been considered as catalysts for CO₂ chemical conversion,⁸ it is still necessary to construct more effective MOFs for such reaction especially under mild reaction conditions in order to lower the energy consumption and production costs. Moreover, the factors such as the framework affinity toward CO₂ and the pore-size effect to the substrates still need to be well investigated during the processes of MOF-based CO₂ catalytic conversion. Herein, we present successful fabrication of a highly porous MOF, {Cu₄[(C₅H₃N₁₂) (COO)₈]}_n (**1**),⁹ that incorporates both unsaturated Cu sites and accessible nitrogen-rich triazole units exhibiting a high affinity to CO₂, which shows remarkably high efficiency on catalytic CO₂ cycloaddition with small epoxides at 1 atm and room temperature. The MOF showed a sharp decrease of its activity to larger substrates at the same conditions, indicating its high selectivity toward the size of the substrates.

An inherent structural feature of MOFs distinct from other inorganic porous materials is that they have decorative organic moieties that endow them with chemical tunability by introducing functional groups. Theoretical and experimental investigations have demonstrated that accessible nitrogen-donor groups, such as amine, pyridine, imidazole, triazole, and tetrazole, in the porous materials have a high affinity to CO₂ molecule.^{10–12} Versatile “click chemistry” can easily afford the formation of nitrogen-rich triazole rings with high yield under mild conditions, with which various functional materials have been fabricated.^{12,13} Taking these advantages into account, a nitrogen-rich octacarboxylate ligand, 5,5',5'',5'''-((methanetetrayl)tetrakis-(benzene-4,1-diyl)) tetrakis (1*H*-1,2,3-triazole-4,1-diyl) tetraiso-phthalic acid (**H₈L1**), was successfully synthesized via the

Received: December 21, 2015

Published: February 5, 2016

“click” reaction and subsequent deprotection (see the [Supporting Information \(SI\)](#) for details). Some studies have also revealed that unsaturated metal sites incorporated into MOFs not only dramatically increase the affinity to CO₂ but also act as Lewis acid catalytic centers.^{8d–g,i} On account of easy generation of unsaturated paddlewheel Cu₂ units, Cu(II) ion was selected for the MOF construction with H₈L1, and high quality blue crystals of **1** ([Figure S1](#)) were successfully obtained after solvothermal reaction.

Single-crystal X-ray diffraction analysis reveals that **1** is a three-dimensional (3D) porous network with a framework formula of [Cu₄(L1)]_n ([Figures 1a and S2](#)). As illustrated in [Figure 1b](#), two

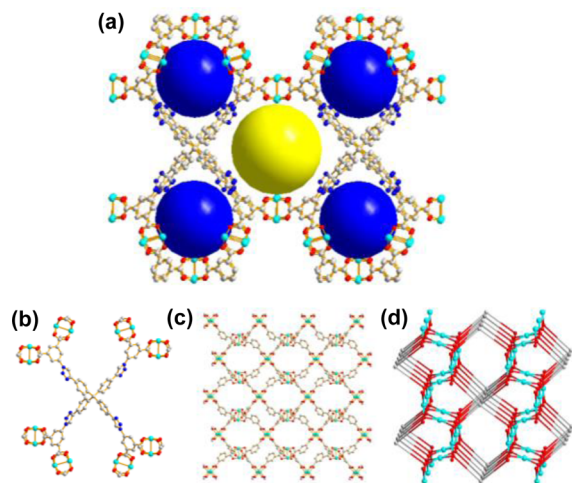


Figure 1. (a) Perspective view of 3D porous framework of **1** showing the incorporation of unsaturated Cu₂ sites and accessible nitrogen-rich triazole groups with two kinds of pores (yellow and blue balls). (b) Coordination of clicked octacarboxylate ligand L1 and unsaturated paddlewheel Cu₂ units. (c) Lamellar framework with regularly located Cu₂ sites connected by isophthalate moieties from L1. (d) Illustration of the (4,3,4)-connected network of **1**.

neighboring Cu(II) ions are bridged by four distributed carboxylate groups from four different L1 ligands to form a paddlewheel Cu₂ cluster.^{12,14} Two neighboring Cu₂ clusters are then bridged by the short linker, isophthalate moiety of L1, giving the formation of a Cu₂ cluster pair that connects with each other to construct two-dimensional (2D) parallel layers with the paddlewheel Cu₂ clusters arranged regularly in quadrilateral geometries ([Figure 1c](#)). Finally, each L1 connecting four pairs of isophthalate-bridged Cu₂ cluster pairs from the 2D layers makes **1** into a (4,3,4)-connected network with “clicked” nitrogen-rich triazole rings uniformly located between paddlewheel Cu₂ constructed layers.¹⁵ The regular combination of the paddlewheel Cu₂ clusters and nitrogen-rich triazole-containing L1 endows **1** with a high porosity, having two kinds of pores in diameters of 7.9 and 12.6 Å, respectively. After removing the discrete and coordinated solvent molecules in the framework, the MOF structure was calculated using PLATON/VOID program.¹⁶ The total solvent-accessible volume of **1** was estimated to be 63.3%, and the density of the desolvated framework was calculated to be 0.762 g cm⁻³, further indicating that **1** possesses a high porosity. The structural analysis and calculations clearly reveal that **1** has a highly porous framework incorporated with both exposed metal sites and coordination-free nitrogen-rich triazole units.

N₂ adsorption measurements were carried out to confirm the porosity. The MOF was degassed under vacuum after being thoroughly soaked by dichloromethane. The powder X-ray diffraction (PXRD) pattern of the activated sample presents a good agreement with calculated PXRD pattern from its crystal data ([Figure S3](#)), indicating that the framework was retained after the activation. Then, the activated sample of **1** was subjected to nitrogen sorption at 77 K. As illustrated in [Figure 2a](#), **1** exhibits

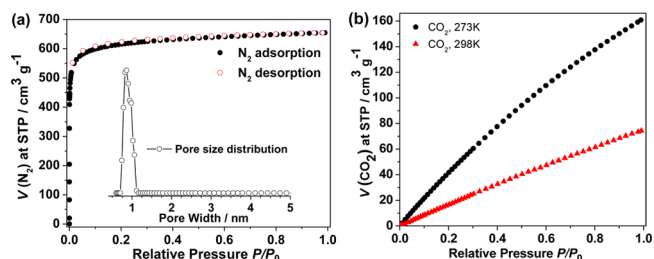


Figure 2. (a) N₂ adsorption/desorption isotherms of **1** at 77 K and its pore size distribution calculated from the isotherms. (b) CO₂ adsorption isotherms at 273 and 298 K, respectively.

reversible type I sorption isotherms with a quickly increased step prior to the plateau, demonstrating that it possesses a microporous feature.¹⁷ The overall N₂ uptake of **1** is 655 cm³ g⁻¹ at 1 atm, and its Brunauer–Emmett–Teller (BET) surface area was calculated to be 2436 m² g⁻¹ ([Figure S5](#)), which is comparable with reported MOFs having similar structures such as NTU-111^{12b} and ZJU-5.^{14b} The calculations based on the N₂ sorption isotherm at 77 K with the nonlocal density functional theory were also carried out to reveal that its pore size distribution ranges from 0.75 to 1.11 Å ([Figure 2a](#)). The pore size distribution is consistent with the observation from its crystal structure. N₂ sorption investigation further confirms that **1** is a highly porous MOF.

High porosity together with the incorporation of exposed metal sites and nitrogen-rich triazole units within the framework of **1** inspired us to investigate its affinity toward CO₂. First, the CO₂ sorption capability of **1** was evaluated. As shown in [Figure 2b](#), **1** shows a CO₂-uptake value of 160.8 cm³ g⁻¹ at 273 K and 1 atm, which is higher than reported MOFs possessing similar surface areas and even comparable with some highly porous MOFs. For example, SNU-50', 77H, NTU-111, NTU-112, and NTU-113 showed CO₂-uptake values of 120.0, 41.8, 124.6, 158.5, and 166.8 cm³ g⁻¹ under the same conditions, having their BET surface areas of 2300, 3670, 2450, 2992, and 3095 m² g⁻¹, respectively.^{12b,18} The high CO₂ uptake should be attributed to the successful introduction of exposed metal sites and nitrogen-rich triazole units into the framework of **1**.¹² Then, the isosteric heat of adsorption (Q_{st}) for CO₂ capture was calculated based on the adsorption isotherms at 273 and 298 K ([Figure 2b](#) and [S6](#)) through the Clausius–Clapeyron equation.^{1c} It was found that the Q_{st} value of **1** for CO₂ sorption is ~32.2 kJ mol⁻¹ at low loading range, followed by the convergence into a pseudoplateau at Q_{st} of ~25.8 kJ mol⁻¹ with relatively high uptake. The Q_{st} is also comparable to some reported nitrogen-rich MOFs such as NTU-105 (~35 kJ mol⁻¹ at low loading range and ~24 kJ mol⁻¹ at relatively high uptake),^{12a} confirming that the constructed MOF **1** has a high affinity to CO₂.

Raman spectroscopy has recently been employed to study MOF properties via spectroscopic changes before and after gas adsorption.¹⁹ Therefore, *in situ* Raman spectral measurements were implemented to **1** in order to monitor its affinity toward

CO₂ molecule. As shown in Figure 3, a new peak for **1** appears at 1377 cm⁻¹ after adsorbing CO₂. While this peak is weaker and

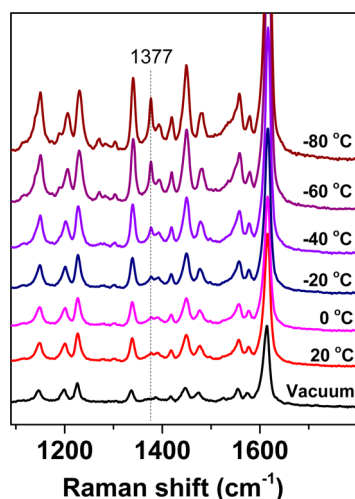
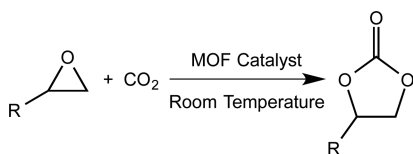


Figure 3. Temperature-dependent Raman spectra of **1** (vacuum) and CO₂-adsorbed **1** (20 to -80 °C) showing obvious spectroscopic changes before and after the CO₂ adsorption of **1**.

broader at room temperature, it becomes much clearer and sharper at lower temperatures. The generated peak should correspond to CO₂ adsorbed in the framework by showing the symmetric C=O stretch mode of CO₂ based on the literature description.¹⁹ The peak position is red-shifted by ~11 cm⁻¹ as compared with the reported value for gaseous CO₂ at 1388 cm⁻¹. The peak shift should be due to the interaction between adsorbed CO₂ and the framework of **1**. Thus, the framework affinity to CO₂ is indisputably evidenced by Raman spectroscopic investigations.

The inherent CO₂-adsorbing property and embedded Lewis acid metal sites in the framework suggest that MOF **1** should be a highly promising heterogeneous catalyst for CO₂ related reactions. Among CO₂ chemical conversion reactions, catalyzed CO₂ cycloaddition with epoxides has been intensively investigated due to wide applications of the produced carbonates in pharmaceutical and electrochemical industries.^{8,20} Therefore, catalytic performance of **1** in the cycloaddition of CO₂ with epoxides to produce various carbonates (Scheme 1) was

Scheme 1. Catalytic Cycloaddition of CO₂ with Epoxides to Produce Cyclic Carbonates



explored. As a benchmark MOF with the same embedded Lewis acid metal sites (exposed paddlewheel Cu₂ clusters), HKUST-1 was also taken as a catalyst in these heterogeneous reactions as control experiments.^{14a}

Yields of the obtained cyclic carbonates produced from CO₂ with related epoxides catalyzed by **1** and HKUST-1 were determined under 1 atm CO₂ pressure at room temperature for 48 h. As shown in Figure 4 and Table S2, the reaction yields catalyzed by **1** from related epoxides are 96% for 2-methyloxirane, 83% for 2-ethyloxirane, 85% for 2-

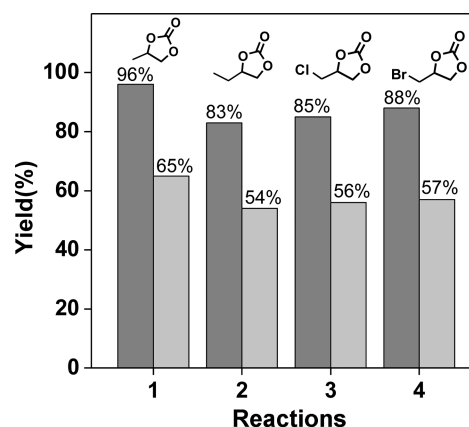


Figure 4. Yields of various cyclic carbonates prepared from the cycloaddition of CO₂ with related epoxides catalyzed by MOF **1** (black) and HKUST-1 (gray). The reaction was conducted in a Schlenk tube using epoxide (20 mmol) with CO₂ purged at 1 atm under a solvent-free environment at room temperature, catalyzed by 0.2 mol % per copper paddlewheel unit of MOF with a cocatalyst of tetra-*n*-tertbutylammonium bromide (0.65 g, 10 mol %) for 48 h.

(chloromethyl)oxirane, and 88% for 2-(bromomethyl)oxirane with corresponding turnover frequency (TOF) values of 200.0, 172.9, 177, and 183.3 h⁻¹ per paddlewheel Cu₂ cluster. For comparison, the yields are 65%, 54%, 56%, and 57% catalyzed by HKUST-1 with TOF values of 135.4, 112.5, 116.7, and 118.8 h⁻¹ per Cu₂ cluster, respectively. The comparison of the yields for all four products clearly reveals that the triazole-containing **1** shows remarkably higher performance than HKUST-1 for catalytic CO₂ cycloaddition with epoxides at the same conditions. Given similar pore size and the same embedded Lewis acid metal sites in both **1** and HKUST-1, the high catalytic activity of **1** should be ascribed to the increase of the CO₂ affinity via the introduction of the nitrogen-rich triazole groups into the framework. Taking the catalytic CO₂ cycloaddition with propylene oxide to produce propylene carbonate as an example, the recyclability was tested by using recycled catalyst **1** collected by centrifugation. No significant decrease in catalytic activity was observed even after 5 runs of the same reactions (Figure S9). The stability of **1** was also proven by the PXRD measurements, showing that the PXRD patterns of the recycled **1** are in good agreement with calculated pattern from its crystal data (Figure S10). The PXRD results indicate that the framework was retained very well after the catalytic reactions. Based on previous reports,⁸ possible MOF-based catalytic mechanism is discussed in the SI (Figure S11). The high activity and recyclability make MOF **1** an excellent heterogeneous catalyst for carbon fixation via CO₂ chemical conversion reactions.

Then, we extended this work to larger epoxide substrates in order to check the generality for such CO₂ cycloaddition reactions. Since the experiments were conducted under solvent-free conditions, three large liquid substrates were selected (Table S2). When 1,2-epoxyoctane, 1,2-epoxydodecane, and 2-ethylhexyl glycidyl ether were employed, the product yields showed sharp decreases in the same conditions. They were just 8%, 6%, and 5% (entries 5–7 in Table S2), respectively, suggesting that large substrates cannot enter into the porous framework of **1** for catalyzed reactions. These observations also indicate that the former reactions of small substrates (entries 1–4 in Table S2) were carried out within the framework of **1**, and the MOF exhibits the size selectivity to small and large substrates in the

reactions. Thus, remarkably high efficiency and the size selectivity to small epoxides on catalytic CO₂ cycloaddition confirm that MOF 1 is a suitable heterogeneous catalyst for carbon fixation.

In summary, we have synthesized a triazole-containing octacarboxylate linker by versatile “click chemistry”, and subsequently it has been utilized for the construction of a highly porous MOF with Cu ions. The constructed MOF incorporating both exposed metal sites and nitrogen-rich triazole groups presents a high affinity to CO₂, which has been clearly verified by gas adsorption and Raman spectral detections. The inherent CO₂ adsorbability, the exposed Lewis acid metal sites, and the confinement of the pore size make the MOF a promising heterogeneous catalyst for CO₂ chemical conversion with small substrates, which have been confirmed by remarkably high efficiency and size selectivity on catalytic CO₂ cycloaddition with epoxides. This research sheds light on how the framework affinity of MOFs to CO₂ and the pore size dependence toward substrates could influence the efficiency of CO₂ chemical conversion during the process of the carbon fixation.

■ ASSOCIATED CONTENT

Supporting Information

The Supporting Information is available free of charge on the ACS Publications website at DOI: 10.1021/jacs.5b13335.

Experimental details. CCDC 1436567 (PDF)

Crystallographic data (CIF)

■ AUTHOR INFORMATION

Corresponding Authors

*zhaoyanli@ntu.edu.sg

*rzou@pku.edu.cn

Author Contributions

§These authors contributed equally.

Notes

The authors declare no competing financial interest.

■ ACKNOWLEDGMENTS

This research was financially supported by the National Research Foundation (NRF), Prime Minister's Office, Singapore through its Campus for Research Excellence and Technological Enterprise (CREATE) Program—Singapore Peking University Research Centre for a Sustainable Low-Carbon Future. R.Z. thanks the National Natural Science Foundation of China (nos. 51322205, 21371014, and 11175006) for the financial support.

■ REFERENCES

- (1) (a) Li, J.-R.; Ma, Y.; McCarthy, M. C.; Sculley, J.; Yu, J.; Jeong, H.-K.; Balbuen, P. B.; Zhou, H.-C. *Coord. Chem. Rev.* **2011**, *255*, 1791. (b) Bae, Y.-S.; Snurr, R. Q. *Angew. Chem., Int. Ed.* **2011**, *50*, 11586. (c) Sumida, K.; Rogow, D. L.; Mason, J. A.; McDonald, T. M.; Bloch, E. D.; Herm, Z. R.; Bae, T.-H.; Long, J. R. *Chem. Rev.* **2012**, *112*, 724. (d) Liu, J.; Thallapally, P. K.; McGrail, B. P.; Brown, D. R.; Liu, J. *Chem. Soc. Rev.* **2012**, *41*, 2308.
- (2) (a) Gomes, C. D. N.; Jacquet, O.; Villiers, C.; Thuery, P.; Ephritikhine, M.; Cantat, T. *Angew. Chem., Int. Ed.* **2012**, *51*, 187. (b) Lu, X.-B.; Darenbourg, D. J. *Chem. Soc. Rev.* **2012**, *41*, 1462.
- (3) (a) Iizuka, K.; Wato, T.; Miseki, Y.; Saito, K.; Kudo, A. *J. Am. Chem. Soc.* **2011**, *133*, 20863. (b) Xie, Y.; Wang, T.-T.; Liu, X.-H.; Zou, K.; Deng, W.-Q. *Nat. Commun.* **2013**, *4*, 1960. (c) Tu, W.; Zhou, Y.; Zou, Z. *Adv. Mater.* **2014**, *26*, 4607. (d) Lin, S.; Diercks, C. S.; Zhang, Y.-B.; Kornienko, N.; Nichols, E. M.; Zhao, Y.; Paris, A. R.; Kim, D.; Yang, P.; Yaghi, O. M.; Chang, C. J. *Science* **2015**, *349*, 1208.

(4) (a) Sculley, J.; Yuan, D.; Zhou, H.-C. *Energy Environ. Sci.* **2011**, *4*, 2721. (b) Suh, M. P.; Park, H. J.; Prasad, T. K.; Lim, D.-W. *Chem. Rev.* **2012**, *112*, 782.

(5) (a) He, Y.; Zhou, W.; Yildirim, T.; Chen, B. *Energy Environ. Sci.* **2013**, *6*, 2735. (b) He, Y.; Zhou, W.; Qian, G.; Chen, B. *Chem. Soc. Rev.* **2014**, *43*, 5657.

(6) (a) Xiang, S.-C.; Zhang, Z.; Zhao, C.-G.; Hong, K.; Zhao, X.; Ding, D.-R.; Xie, M.-H.; Wu, C.-D.; Das, M. C.; Gill, R.; Thomas, K. M.; Chen, B. *Nat. Commun.* **2011**, *2*, 204. (b) Wu, H.; Gong, Q.; Olson, D. H.; Li, J. *Chem. Rev.* **2012**, *112*, 836.

(7) (a) Zhang, T.; Lin, W. *Chem. Soc. Rev.* **2014**, *43*, 5982. (b) Chughtai, A. H.; Ahmad, N.; Younus, H. A.; Laypkov, A.; Verpoort, F. *Chem. Soc. Rev.* **2015**, *44*, 6804.

(8) (a) Song, J.; Zhang, Z.; Hu, S.; Wu, T.; Jiang, T.; Han, B. *Green Chem.* **2009**, *11*, 1031. (b) Miralda, C. M.; Macias, E. E.; Zhu, M.; Ratnasamy, P.; Carreon, M. A. *ACS Catal.* **2012**, *2*, 180. (c) Zhou, X.; Zhang, Y.; Yang, X.; Zhao, L.; Wang, G. *J. Mol. Catal. A: Chem.* **2012**, *361–362*, 12. (d) Cho, H.-Y.; Yang, D.-A.; Kim, J.; Jeong, S.-Y.; Ahn, W.-S. *Catal. Today* **2012**, *185*, 35. (e) Zalomaeva, O. V.; Chibiryaev, A. M.; Kovalenko, K. A.; Kholdeeva, O. A.; Balzhinimaev, B. S.; Fedin, V. P. *J. Catal.* **2013**, *298*, 179. (f) Feng, D.; Chung, W.-C.; Wei, Z.; Gu, Z.-Y.; Jiang, H.-L.; Chen, Y.-P.; Darenbourg, D. J.; Zhou, H.-C. *J. Am. Chem. Soc.* **2013**, *135*, 17105. (g) Gao, W.-Y.; Chen, Y.; Niu, Y.; Williams, K.; Cash, L.; Perez, P. J.; Wojtas, L.; Cai, J.; Chen, Y.-S.; Ma, S. *Angew. Chem., Int. Ed.* **2014**, *53*, 2615. (h) Beyzavi, M. H.; Klet, R. C.; Tussupbayev, S.; Borycz, J.; Vermeulen, N. A.; Cramer, C. J.; Stoddart, J. F.; Hupp, J. T.; Farha, O. K. *J. Am. Chem. Soc.* **2014**, *136*, 15861. (i) Zheng, J.; Wu, M.; Jiang, F.; Su, W.; Hong, M. *Chem. Sci.* **2015**, *6*, 3466. (j) Han, X.; Wang, X.-J.; Li, P.-Z.; Zou, R.; Li, M.; Zhao, Y. *CrystEngComm* **2015**, *17*, 8596.

(9) MOF 1 in the main text can be cited as NTU-180.

(10) (a) Vogiatzis, K. D.; Mavrandonakis, A.; Klopffer, W.; Froudakis, G. E. *ChemPhysChem* **2009**, *10*, 374. (b) Li, P.-Z.; Zhao, Y. *Chem. - Asian J.* **2013**, *8*, 1680.

(11) (a) Vaidyanathan, R.; Iremonger, S. S.; Shimizu, G. K. H.; Boyd, P. G.; Alavi, S.; Woo, T. K. *Science* **2010**, *330*, 650. (b) Zheng, B.; Bai, J.; Duan, J.; Wojtas, L.; Zaworotko, M. J. *J. Am. Chem. Soc.* **2011**, *133*, 748.

(12) (a) Wang, X.-J.; Li, P.-Z.; Chen, Y.; Zhang, Q.; Zhang, H.; Chan, X. X.; Ganguly, R.; Li, Y.; Jiang, J.; Zhao, Y. *Sci. Rep.* **2013**, *3*, 1149. (b) Li, P.-Z.; Wang, X.-J.; Zhang, K.; Nalaparaju, A.; Zou, R.; Zou, R.; Jiang, J.; Zhao, Y. *Chem. Commun.* **2014**, *50*, 4683.

(13) (a) Nnagai, A.; Guo, Z.; Feng, X.; Jin, S.; Chen, X.; Ding, X.; Jiang, D. *Nat. Commun.* **2011**, *2*, 536. (b) Liu, C.; Li, T.; Rosi, N. L. *J. Am. Chem. Soc.* **2012**, *134*, 18886. (c) Li, P.-Z.; Wang, X.-J.; Tan, S. Y.; Ang, C. Y.; Chen, H.-Z.; Liu, J.; Zou, R.-Q.; Zhao, Y. *Angew. Chem., Int. Ed.* **2015**, *54*, 12748.

(14) (a) Chui, S. S.-Y.; Lo, S. M.-F.; Charmant, J. P. H.; Orpen, A. G.; Williams, I. D. *Science* **1999**, *283*, 1148. (b) Rao, X.; Cai, J.; Yu, J.; He, Y.; Wu, C.; Zhou, W.; Yildirim, T.; Chen, B.; Qian, G. *Chem. Commun.* **2013**, *49*, 6719.

(15) (a) Perry, J. J., IV; Perman, J. A.; Zaworotko, M. J. *Chem. Soc. Rev.* **2009**, *38*, 1400. (b) Janiak, C.; Vieth, J. K. *New J. Chem.* **2010**, *34*, 2366. (c) Li, M.; Li, D.; O'Keeffe, M.; Yaghi, O. M. *Chem. Rev.* **2014**, *114*, 1343.

(16) Spek, A. *Acta Crystallogr., Sect. D: Biol. Crystallogr.* **2009**, *65*, 148.

(17) Sing, K. S. W.; Everett, D. H.; Haul, R. A. W.; Moscou, L.; Pierotti, P. A.; Rouquerol, J.; Siemieniewska, T. *Pure Appl. Chem.* **1985**, *57*, 603.

(18) Prasad, T. K.; Hong, D. H.; Suh, M. P. *Chem. - Eur. J.* **2010**, *16*, 14043.

(19) (a) Nijem, N.; Thissen, P.; Yao, Y.; Longo, R. C.; Roodenko, K.; Wu, H.; Zhao, Y.; Cho, K.; Li, J.; Langreth, D. C.; Chabal, Y. J. *J. Am. Chem. Soc.* **2011**, *133*, 12849. (b) Kanoo, P.; Reddy, S. K.; Kumari, G.; Haldar, R.; Narayana, C.; Balasubramanian, S.; Maji, T. K. *Chem. Commun.* **2012**, *48*, 8487.

(20) North, M.; Pasquale, R.; Young, C. *Green Chem.* **2010**, *12*, 1514.